European Journal of Cardio-Thoracic Surgery 46 (2014) 767–778
doi:10.1093/ejcts/ezu242 Advance Access publication 26 June 2014

REVIEW

Bioprinting of artificial blood vessels: current approaches towards a demanding goal

Eva Hoch[a], Günter E.M. Tovar[a,b,*] and Kirsten Borchers[b,*]

[a] Institute for Interfacial Process Engineering and Plasma Technology IGVP, University of Stuttgart, Stuttgart, Germany
[b] Fraunhofer Institute for Interfacial Engineering and Biotechnology IGB, Stuttgart, Germany

* Corresponding author. Fraunhofer Institute for Interfacial Engineering and Biotechnology IGB, Nobelstr. 12, 70569 Stuttgart, Germany. Tel: +49-711-9704121; fax: +49-711-9704200; e-mail: kirsten.borchers@igb.fraunhofer.de (K. Borchers); Institute for Interfacial Process Engineering and Plasma Technology IGVP, University of Stuttgart, Nobelstr. 12, 70569 Stuttgart, Germany . Tel: +49-711-9704109 ; fax: +49-711-9704200; e-mail: guenter.tovar@igvp.uni-stuttgart.de (G. Tovar).

Received 6 May 2014; accepted 8 May 2014

Summary

Free-form fabrication techniques, often referred to as '3D printing', are currently tested with regard to the processing of biological and biocompatible materials in general and for fabrication of vessel-like structures in particular. Such computer-controlled methods assemble 3D objects by layer-wise deposition or layer-wise cross-linking of materials. They use, for example, nozzle-based deposition of hydrogels and cells, drop-on-demand inkjet-printing of cell suspensions with subsequent cross-linking, layer-by-layer cross-linking of synthetic or biological polymers by selective irradiation with light and even laser-induced deposition of single cells. The need of vessel-like structures has become increasingly crucial for the supply of encapsulated cells for 3D tissue engineering, or even with regard to future application such as vascular grafts. The anticipated potential of providing tubes with tailored branching geometries made of biocompatible or biological materials pushes future visions of patient-specific vascularized tissue substitutions, tissue-engineered blood vessels and bio-based vascular grafts. We review here the early attempts of bringing together innovative free-form manufacturing processes with bio-based and biodegradable materials. The presented studies provide many important proofs of concepts such as the possibility to integrate viable cells into computer-controlled processes and the feasibility of supplying cells in a hydrogel matrix by generation of a network of perfused channels. Several impressive results in the generation of complex shapes and high-aspect-ratio tubular structures demonstrate the potential of additive assembly methods. Yet, it also becomes obvious that there remain major challenges to simultaneously match all material requirements in terms of biological functions (cell function supporting properties), physicochemical functions (mechanical properties of the printed material) and process-related (viscosity, cross-linkability) functions, towards the demanding goal of biofabricating artificial blood vessels.

Keywords: Bioprinting • Tissue engineering • Artificial blood vessels

INTRODUCTION

Tissue engineering (TE) aims for the *in vitro* generation of functional, artificial tissues and organs, which may serve as implants *in vivo* [1] or as *in vitro* test systems [2–4]. In the classical approach, cells are seeded onto 3D matrices [1] that are either bio-based such as decellularized donor tissue [5–8] or synthetic materials fabricated by electrospinning, freeze drying, foaming or rapid prototyping technologies [9–12]. Another strategy is the encapsulation of cells into 3D hydrogels [13–15]. Based on these techniques, simple and thin tissue mimics of, for example, skin [16, 17], cartilage [4, 18, 19] or cornea [20] have been realized, partially with the help of special perfusing bioreactors [21, 22]. Yet, the size of engineered tissues is restricted due to the inability to incorporate a sufficient blood vessel system for nutrient and oxygen supply to the cells [23].

The native vascular system is a complex network of blood vessels of various sizes. The diameters of blood vessels range from the centimetre to the micrometre scale, i.e. from ∼2.5 cm to ∼20 μm for the aorta to very fine capillaries, respectively [24]. The inner face of the whole vascular system is lined with a monolayer of flat cells, the endothelial cells (ECs). This EC layer prevents thrombogenesis in the blood flow and represents a cellular barrier that controls the exchange of molecules from blood and tissue. Branching of vessels occurs consistent with certain rules that guarantee haemostasis, for example, perpetuation of a homogeneous wall shear stress [25]. The maximum distance between two capillaries is 200 μm, which correlates to the diffusion limitation of oxygen [23].

With a view to the generation of larger artificial tissue and implantation of tissue into patients, current research focuses on the *in vitro* generation of functional, artificial blood vessel systems. Additionally, the lack of small-diameter vascular grafts motivates the search for technologies and materials to provide biomimetic vascular structures for new generative therapies.

As one possible approach, cell-based strategies focus on the promotion of angiogenesis by (self-)assembly of vascular cells. For example Moya *et al.* have recently demonstrated the assembly of ECs to form an interconnected and perfusable human capillary network as part of a microfluidic device as they adjusted adequate

pressure drops between 'arterial' and 'venular' channels [26]. Their combination of defined inlet and outlet branches as provided by the microfluidic device with the formation of a genuine capillary network within the device enabled perfused vascular networks *in vitro*, but in its current form is not useful for the assembly of 3D tissue or implantation into living organisms. With respect to *in vivo* application of artificial tissue, it has a been observed in early studies by Tremblay *et al*. [27] and has also been acknowledged in recent studies performed, for example, by Nunes *et al*. [28] that tissue structures containing fragments of capillaries connected much faster to the native vascular system of a host upon implantation than tissue without such vascular prestructures. Yet, such constructs, on the other hand, do not provide continuous tubular vessel systems *in vitro* and, therefore, they cannot be used for the supply of surrounding cells as needed for 3D TE.

Thus, the essential requirements for fabrication of perfusable vascularized tissue seem to be both, to have defined inlet and outlet branches and to provide a capillary-like network with biomimetic vessel geometry for undisturbed fluid dynamics [29].

Therefore, additional approaches provide ready-made tubes or tubular networks as a 3D matrix for supplying cells in 3D culture. These may be either based on the reuse of biologically derived, decellularized vessel systems [30] or synthetically manufactured tubular scaffolds [31]. To develop artificial structures that perform as well as natural ones, we need fabrication processes that do not set any limits to the generation of structures and shapes, and materials that allow for tailoring of their physical, chemical and biological properties. Bioprinting technology, which applies free-form fabrication methods to deposit scaffold materials and cells to form digitally defined 3D structures [32], constitutes a basically novel approach to approach this so far unsolved issue: There are various types of 3D manufacturing techniques addressing a broad range of structure sizes and several have already been used for biofabrication purposes as well.

THE POTENTIAL OF BIOPRINTING TECHNIQUES

Bioprinting means the generation of bioengineered structures by additive manufacturing of biological and biologically relevant materials with the use of computer-aided transfer and build-up processes [33–35]. A variety of solid freeform fabrication techniques are available. They can be divided into laser-based methods, printer-based methods and nozzle-based methods.

Nozzle-based systems use pressure-assisted syringes to deposit continuous strands of materials. They typically address structure sizes in the centimetre range with resolutions of several hundred microns [36]. Printer-based systems include thermal and piezoelectric inkjet printing. These drop-on-demand systems generate small droplets of low viscosity 'bio' ink [37]. Typical resolutions are in the range of ~85–300 µm and can be used for generation of millimetre to centimetre constructs [35]. Laser-based systems including stereolithography and multiphoton polymerization as well as digital light processing (DLP), a method based on digital micromirror devices [38], use light for site-selective curing of photosensitive prepolymers in a bath with resolutions down to the sub-micron range [39].

Three parallel bioprinting-based approaches are followed towards the aim of the generation of artificial blood vessels: (i) generation of bulk matrices with integrated channels as perfusable matrices, (ii) cell patterning into line structures for self-assembly of interconnected vessel systems and (iii) generation of free-standing tubular structures, with and without encapsulated cells, which may serve as artificial blood vessels (Table 1).

PERFUSABLE MATRICES

The most straightforward approach to perfusable tissue might be the generation of a network of interconnected channels within the tissue matrix. Such channels may be used as supply system for cells within the surrounding matrix and may additionally be seeded with ECs. Early works used moulds for preparing sacrificial structures in order to fabricate microfluidic networks, which then allowed the transport of macromolecules into surrounding hydrogels under low driving pressure differences. Such studies resulted in zones of high cell viability up to 200 µm away from the perfused channels and thus demonstrate the effectiveness of the strategy. Yet, the soft lithographic techniques that were applied for channel generation require multiple processing steps and are limited to planar networks and stacks of planar networks [65–67]. Another approach presented by Bellan *et al*. used melt-spun fibres as a sacrificial mould and thus achieved a 3D channel network, yet in random spatial orientation [40].

For rapid casting of a defined pattern of vascular channels, Miller *et al*. developed a sacrificial material based on carbohydrates, which they printed in filaments using a syringe and a RepRap Mendel 3D printer [41]. They used mixtures out of glucose, sucrose and dextran (86 kDa) as 'liquid glass' and produced self-supporting perpendicular lattices as well as curved filaments and Y-junctions with fibre diameters in the range of 150–750 µm (Fig. 1). Such glass lattices were coated with thin layers of poly(lactid-*co*-glycolid) (PLGA) and subsequently encapsulated in the presence of living cells using a wide range of natural and synthetic matrix materials such as fibrin, agarose and Matrigel®, and poly(ethylene glycol) (PEG)-based materials. After cross-linking of the matrix, the carbohydrate support was dissolved in aqueous media. Thereby, the PLGA layer prevented carbohydrate solution from flowing through the cell-laden hydrogel. The resulting channels allowed non-leaking perfusion of human blood. ECs were seeded into the channels and lined the walls of the complete network. The authors observed sprouting of new capillaries from the channel walls into the surrounding fibrin gels which had been laden with 10T1/2 cells. In agarose gels and even in gels made from synthetic PEG hydrogels, which were modified with the RGD cell recognition peptide, various cell types were live and active at the gel perimeter and approximately 1 mm around the perfusion channels. For comparison, within gels without channels, cells were only active at the gel slab perimeter but not at the gel core.

Lee *et al*. dispensed heated gelatin solution for the generation of sacrificial elements and ice-cooled collagen hydrogel precursor at a pH of 4.5 to produce collagen layers, which were then cross-linked by spraying $NaHCO_3$ solution on top [43]. Dermal fibroblasts grown in such collagen scaffolds containing fluidic channels also showed significantly elevated cell viability compared with the ones without any channels, proving again the effectiveness of integrating vascular structures for 3D tissue reconstruction.

In their approach to fabricate a free-form 3D channel network within a hydrogel, Wu *et al*. used a reservoir of photo-cross-linkable, acrylated Pluronic F127® (PF127, 20–25% w/w) and deposited sacrificial filament networks from nonacrylated PF127 directly into such reservoirs [42]. PL127 is an interesting material for manufacturing purposes because it shows unusual properties, i.e., it is liquid at 4°C and solidifies when warmed. It is one of the

Table 1: Overview over biofabrication methods and materials used in present approaches for the generation of vascular structures

Bioprinting technique	Building material/bulk hydrogel	Sacrificial material/supportive material	Cell type	Channel diameter	Ref.
Perfusable matrices					
Nozzle-based: Modified cotton candy machine	Enzymatically cross-linked gelatin	Shellac	–	Diameter: 17 ± 19 µm	[40]
Nozzle-based: RepRap Mendel 3D printer	PEG diacrylate + acrylate-PEG-RGDS; Matrigel®; agarose; alginate; fibrin	Carbohydrate glass (glucose + sucrose + dextran)	HUVEC, 10T1/2 cells	Diameters: 150–750 µm, straight and curved channels	[41]
Nozzle-based	Acrylated Pluronic F127®	Pluronic F127®	–	18–1200 µm	[42]
Nozzle-based	Collagen	Gelatin	Primary HDFs	µm to mm range	[43]
Nozzle-based	Mixtures of gelatin, alginate, chitosan, fibrinogen, HA	–	Rat primary hepatocytes, ADSCs	mm range	[44]
Cell patterning for autonomous vessel formation					
Laser-based: BioLP	–	–	HUVEC, HUVSMC	µm range (single-cell positioning)	[45]
Laser-based: BioLP	Alginate, Matrigel®, fibrin	–	Rabbit carcinoma cell line B16, HUVEC cell line Eathy926	µm to mm range	[46]
Drop-on-demand: HP Deskjet 500	Fibrin	–	HMVEC	µm range	[47]
Nozzle-based: BioAssembly Tool	Collagen	–	RFMF	mm range	[48]
Free-standing tubular structures					
Laser-based: Two-photon polymerization	α,ω-Polytetrahydrofuranether-diacrylate	–	–	Diameter: 10–100 µm	[49]
Laser-based: Digital light processing	Formulations based on urethan-diarylate, hydroxyl ethylacrylate as reactive diluent, ethylene glycol bisthioglycolate as the chain transfer agent		–	Diameter: 4 µm Wall: 2 mm Height: 2 mm	[38]
Drop-on-demand: Thermal inkjet, SEAjet™	Alginate	Ca solution + HA/PVA	–	Diameter: 50–1000 µm	[50, 51]
Drop-on-demand: Thermal inkjet, SEAjet™	Alginate	Ca solution + PVA	HeLa	Diameter: 200 µm	[52]
Drop-on-demand: Thermal inkjet, HP697c	Alginate	Alginate solution	Rat SMC	Diameter: 2 mm Wall: 2 mm Height: 2 mm	[53]
Drop-on-demand: Piezoelectric MicroFab MJ-ABL-01-120-6MX dispense head	Alginate	Ca solution	NIH 3T3 fibroblasts		[54]
Drop-on-demand: Custom-made, syringe + switchable valve applied droplet volume of 116 nl	Agarose	Hydrophobic high-density perfluorotributylamine $C_{12}F_{27}N$	Human MG-63 and human MSC	Diameter: ∼7 mm Wall: ∼1.5 mm Height: ∼4 cm	[55]
Nozzle-based: Novogen MMX Bioprinter, Organovo	NovoGel	–	Mouse embryonic fibroblasts		[56]
Nozzle-based: Fab@Home	Thiol-modified HA + thiol-modified gelatin with gold nanoparticles or tetra-acrylated PEG as cross-linker	HA	NIH 3T3 fibroblasts	Diameter: 3–5 mm Wall: 1–2 mm Height: 1–2 cm	[57]
Nozzle-based: Fab@Home	Methacrylated HA + methacrylated gelatin	HA	Human hepatoma cells HepG2 C3A	Diameter: 1–2 mm Wall: 2 mm	[58]

Continued

Table 1: Continued

Bioprinting technique	Building material/bulk hydrogel	Sacrificial material/supportive material	Cell type	Channel diameter	Ref.
Nozzle-based: Fab@Home	Thiol-modified HA + TetraPAc13 (cross-linker)	HA	NIH 3T3 fibroblasts	Diameter: 500 µm Wall: 500 µm	[59]
Nozzle-based: BioScaffolder 3DF system, SYS + ENG, Germany	Polycaprolactone	–	–	Diameter: 2–4 mm Wall: 1 mm Height: 20 mm Total size: 67 × 42 × 8 mm³	[60]
Nozzle-based: BioScaffolder 3DF system SYS + ENG, Germany	Methacrylated gelatin/gellan gum hydrogel	–	–	Diameter: 2–4 mm Wall: 1 mm Height: 20 mm Total size: 67 × 42 × 8 mm³	[60]
Nozzle-based:	Multicellular spheroids	–	HUVSMCs, HDFs	Diameter: 900 µm Wall: 300 µm	[61]
Nozzle-based: Co-axial nozzle printing	Alginate	–	Bovine cartilage progenitor cells	Diameter: ~100–600 µm	[62–64]

ADSCs: adipose-derived stromal cells; HDFs: human dermal fibroblasts; HUVECs: human umbilical vein endothelial cells; 10T1/2; HUVECs: human umbilical vein endothelial cells; HUVSMCs: human umbilical vein smooth muscle cells; HMVECs: human microvascular endothelial cells; RFMFs: rat fat microvessel fragments; HUVSMCs: human umbilical vein smooth muscle cells; MSCs: mesenchymal stem cells; SMCs: smooth muscle cells; HA: hyaluronan; PEG: poly(ethylene glycol); RGDS: arginine–glycine–aspartic acid–serine; BioLP: biological laser printing; DOD: drop-on-demand.

few synthetic polymer materials that are approved for clinical applications by the American Food and Drug Association FDA [68]. However, the presented study does not discuss the integration of cells into the constructs, and other studies revealed non-cytotoxicity of PF127 gels only up to 20%. [69, 70] Therefore, we consider the use of acrylated PF 127 as a cross-linkable matrix material to provide a proof of concept of omnidirectional filament extrusion within a hydrogel precursor matrix rather than a real matrix for 3D TE.

Li *et al*. introduced bio-based material systems that were suited for vertical assembly of hollow channels without the use of a supportive sacrificial material (Fig. 2). The authors used different combinations of mixed gelatin/alginate/chitosan/fibrinogen hydrogels as building materials. Their printed structures were first stabilized by the sol–gel transition of the gelatin as the mixtures (37°C) were extruded from the syringe needle into a low-temperature fabrication chamber (6–8°C). The alginate, chitosan and fibrinogen were then subsequently cross-linked using thrombin, $CaCl_2$, $Na_5P_3O_{10}$ and glutardialdehyde [44].

CELL PATTERNING FOR SELF-ASSEMBLY OF INTERCONNECTED VESSEL SYSTEMS

The second approach to generate blood vessels in artificial tissue deals with the ability of ECs to organize into blood vessels autonomously (angiogenesis). *In vivo* angiogenesis occurs as a response to hypoxia, for example, in growing tissue when ECs sprout from existing blood vessels to form new capillaries by the curling of a single or few cells [71]. While for *in vitro* TE, an interconnected supply system has to be instantaneously available, genuine vascular structures may mature in parallel for the fast integration of the engineered tissue to the host tissue upon implantation. It has been observed that cultivation of ECs that were randomly distributed within 3D, growth factor-rich hydrogels, e.g. Matrigel®, led to formation of an undirected, polygonal cellular network [72]. Thus, it is expected that prestructuring of vascular cells may guide the direction of lumen formation and growth into an interconnected capillary system. By the application of digital patterning techniques, directed cell deposition can be achieved and branching structures with biomimetic branching geometries may be designed.

Towards this aim, biological laser printing (BioLP), also referred to as laser-assisted bioprinting (LAB), allows for deposition of individual cells. This method is based on laser-induced forward transfer of biological materials and cells. Wu and Ringeisen [45] and Guillotin *et al*. [46] used LAB for positioning of individual human umbilical vein endothelial cells (HUVECs). Wu and Ringeisen designed defined branch and stem structures and observed that deposited HUVECs connected with each other within 1 day (Fig. 3). However, the connected branches built from HUVECs alone did not last more than a few days. Stabilization of the cellular network structure for at least 9 days occurred only with the deposition of an additional cell layer of human umbilical vein smooth muscle cells (HUVSMCs) on top of HUVECs. This confirms similar results from other labs and indicates that assembly of ECs with additional vascular cells, such as pericytes and smooth muscle cells, is crucial for the generation of stable, functional artificial blood vessels and functional tissue substitutes [73, 74].

While laser-based technologies allow for precise positioning of individual cells and thereby the generation of structures with resolution at the cellular level, technologies such as inkjet printing or

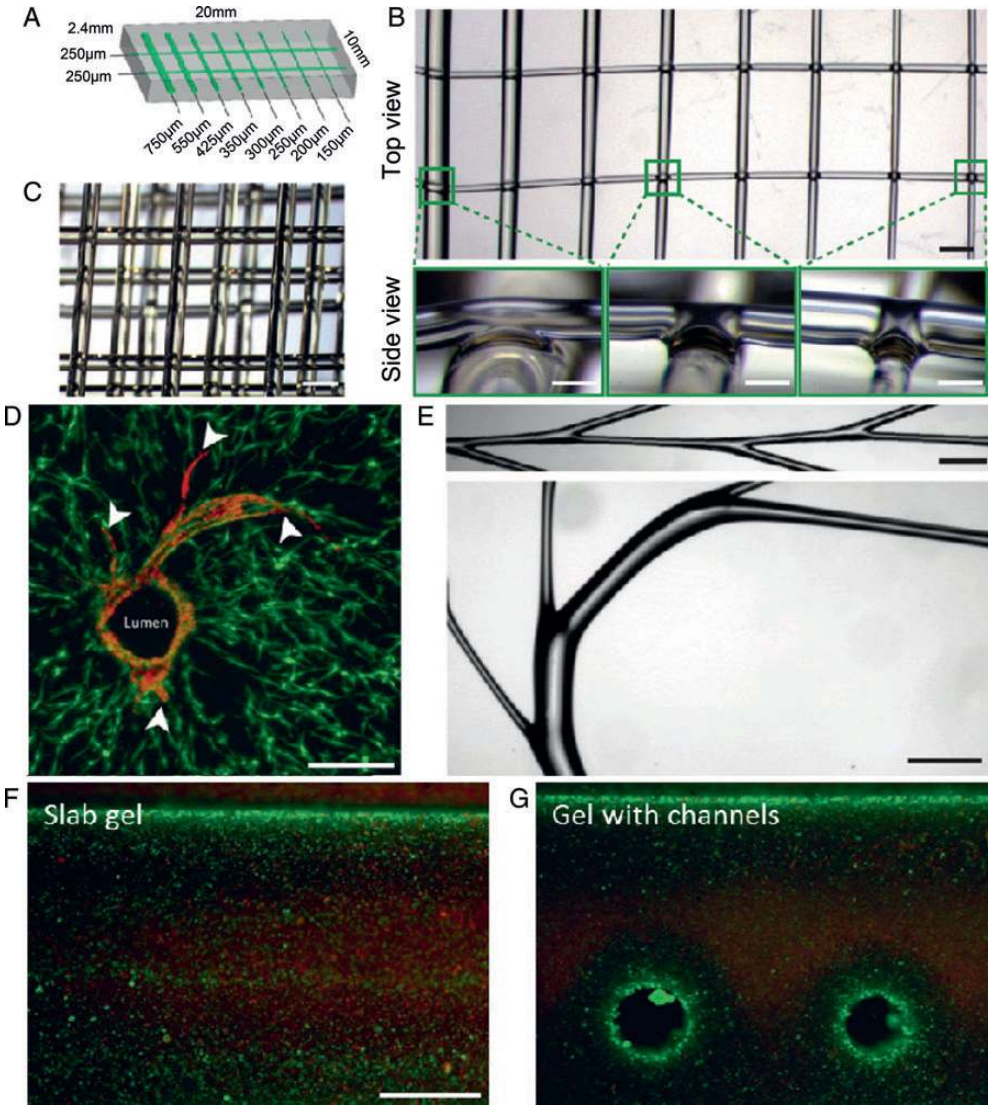

Figure 1: Generation of perfusable channels represents one successful approach to improve cell supply within 3D hydrogel matrices. (**A**) Architectural design of a multiscale lattice (green), (**B**) top view of the design shown in **A** printed in carbohydrate glass, (**C**) multilayered lattices were fabricated in minutes with precise lateral and axial positioning, (**D**) endothelial cells formed single and multicellular sprouts (arrowheads) from patterned vasculature, as seen in a *z*-stack (optical thickness = 200 µm) from within the gel (*z*-position = 300 µm), (**E**) serial *y*-junctions and curved filaments were also fabricated, (**F** and **G**) primary rat hepatocytes and stabilizing stromal fibroblasts in agarose gels (**F**) slab gel, (**G**) channelled gel after 8 days of culture were stained with a fluorescent live/dead assay (green: calcein AM; red: ethidium homodimer): Cells survived at the gel perimeter and near perfused channels, and survival decayed deeper in the gels. Scale bars are 1 mm. (Reproduced and slightly modified from Miller *et al.* [41], with the permission of Nature Publishing Group.)

dispensing enable the generation of structures in the micrometre and millimetre range. Drop-on-demand inkjet printing generates single droplets and can be used to process low viscosity hydrogel precursors (~10 mPa s and below) and cells. Such so-called bioinks are cross-linked after the jetting to form a (bio-)artificial extracellular matrix (ECM) around the printed cells. Cui and Boland, for example from the Boland lab in Texas, which was one of the cradles of bioprinting, built fibrin microstructures laden with human microvascular endothelial cells (HMVECs) using a modified thermal office inkjet printer [47]. They printed droplets of thrombin solution and cells into a bath of fibrinogen on the substrate. The printed HMVECs were found to proliferate within 7 days and align along the printed fibrin gel structure. With their experiment, Cui and Boland proved that thermal inkjet printing can be used for cell and matrix patterning.

Besides isolated ECs, microvessel fragments can also be applied as primary building blocks for autonomous vessel formation via angiogenesis. Chang *et al.* prepared collagen structures in the millimetre range with encapsulated rat fat microvessel fragments (RFMFs) using a nozzle-based 3D bioprinting tool [48]. The narrowed extrusion of the relatively rigid RFMF within a liquid suspension (collagen solution) uniaxially aligned the RFMFs. After 7 days of culture *in vitro* and after subcutaneous implantation into immunocompromised mice, they found that numerous neo-vessels spread from the parent RFMFs and were perfused. However, in the mature network, the initial uniaxial alignment was lost. Conversely, when a uniaxial steel mesh frame was used as patterning cue instead, which maintained tension across the 3D construct also during implantation, the microvessel segments in the mature network were oriented as intended. This experiment indicates that the angioarchitecture is profoundly influenced by mechanical forces that are derived from the surrounding tissue. Such experience suggests that the initial patterning of cells or vascular fragments may not be sufficient when aiming at the generation of

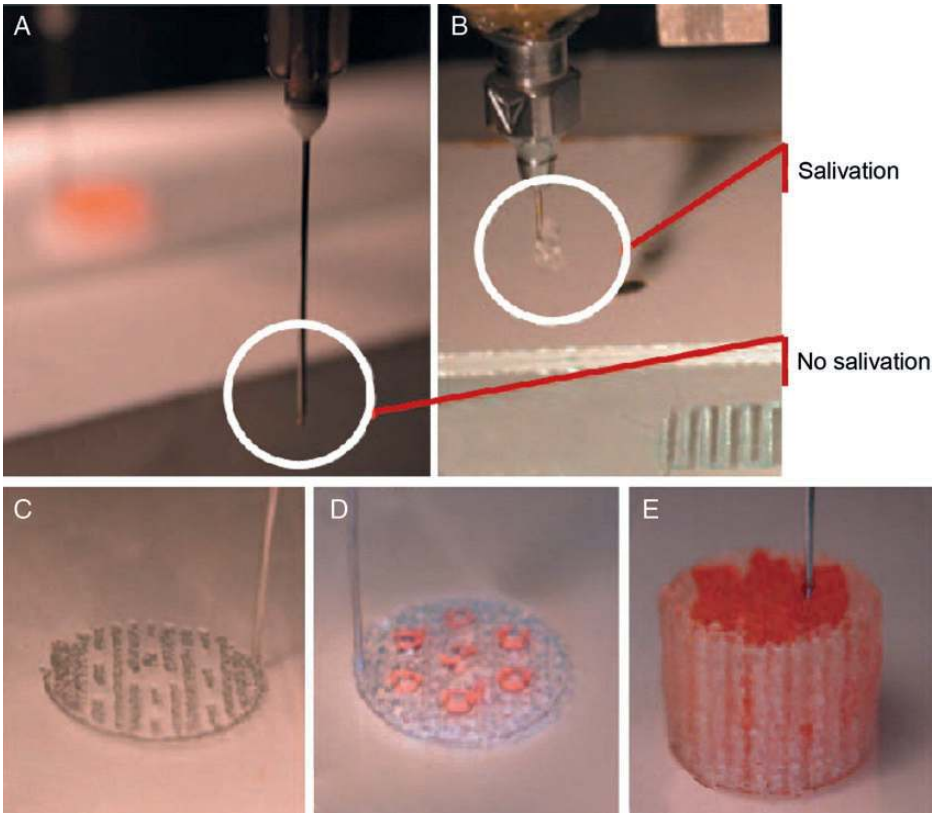

Figure 2: The layer-by-layer assembly of hydrogel mixtures combining the gelling behaviour of gelatin and cross-linking of additional biopolymers such as alginate or fibrinogen enabled generation of vertical channels without the use of a support material. Dispensing of hydrogels with two different types of cells was demonstrated. Red, tube-like part: Adipose-derived stem cells from rat within gelatin/alginate/fibrinogen in DMEM/F12 cell culture media. White, meshwork part: Rat hepatocytes within gelatin/alginate/chitosan in PB; (**A** and **B**) the control of salivation by improved processing intervals; (**C**–**E**) the layer-by-layer fabrication process. (Reproduced from Li *et al*. [44], with the permission of Sage Publications.)

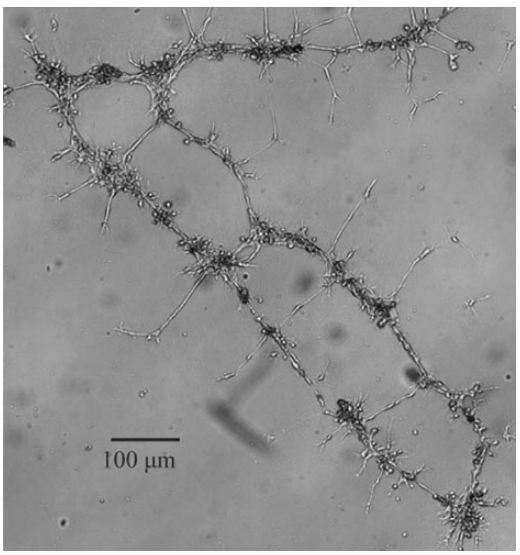

Figure 3: Positioning of single cells was demonstrated by application of laser-assisted bioprinting (LAB): Printed HUVEC double branch structure (parallel), 1 day post-printing. The HUVECs from the two different branches reached across and networked. (Reproduced from Wu *et al*. [45], with the permission of IOP Publishing.)

vascular networks with tailored architectures such as defined inlet and outlet branches. A tailored environment providing adequate stimuli such as perfusion or appropriate stiffness might be necessary.

FREE-STANDING TUBULAR STRUCTURES

The technically most demanding approach to artificial vascular systems deals with fabrication of freestanding tubular structures. Such structures can then serve as artificial blood vessels in 3D tissue models and may also reveal some potential for small-diameter blood vessel medical grafts in the future. Recent studies tackle both paths, the preparation of tubular scaffolds without cells and the preparation of tubular structures, which are composed out of cell–matrix compounds or cell aggregates.

To enable the manufacture of tubular structures, i.e. structures of very high aspect ratio, classically, photo-cross-linking-based additive techniques circumvent the problem of structure support by selectively cross-linking the precursor polymer layer by layer within a reservoir of the polymer resin.

As part of the Fraunhofer BioRap® platform, which is dedicated to the development of additive assembly technologies for biological applications, Engelhardt *et al*. and Meyer *et al*. used stereolithography and two-photon polymerization (TPP) to fabricate tubular structures and bifurcated tubes out of photo-cross-linkable synthetic polymers and biopolymers. Meyer *et al*. presented homologous series of photo-polymerizable α, ω-polytetrahydrofuranether (PTHF)-diacrylate resins, which after photo-curing cover Young's Modulus in the range from 8 to 28 MPa [49]. After appropriate rinsing, extracts of the cross-linked PTHF polymers showed non-cytotoxic characteristics. In another work, the authors introduced resins, which were also tailored for inkjet-printing applications and could be photo-cross-linked into

carboxy-terminated polyacrylate networks [31]. They observed that cell adhesion and proliferation at the carboxy-functional surface of such synthetic materials were improved when the surfaces were more hydrophilic.

Applying TPP, Engelhardt *et al.* generated tiny structures in the range of 10–100 µm applying photo-cross-linkable synthetic polymers as well as polymer–protein hybrid microstructures. They demonstrated freeform fabrication of tubular systems with capillary dimensions using, for example, the above-mentioned PTHF-based materials (Fig. 4A and B) [39, 49]. Owing to the hydrophobic nature of the chosen materials, the shape and mechanical properties of the polymer networks remain unchanged in aqueous environments. Once optimized, this may qualify the material to constitute vascular grafts with improved elasticity, compared with the PTFE-based or polyester-based grafts that are commonly used. For application in TE, the generation of porous walls will be necessary in order to enable substance exchange with the surrounding tissue. By combination of high-resolution TPP with further additive techniques such as inkjet printing or stereolithography, a wide range of structure sizes can be addressed and, thus, this approach is assumed to enable the fabrication of complex geometries for the mimicking of biological functions.

The Liska laboratory in collaboration with Stampfl and colleagues also investigated photo-elastomers and an additive generation of artificial vascular constructs. They presented tubular structures with 3D microstructured wall architectures with high porosity and high interconnectivity, which they produced by microstereolithography out of materials originally presented by Schuster *et al.* [38, 75], thereby demonstrating the potential of the method (Fig. 4C and D). To improve the properties of the materials in view of artificial blood vessels, Baudis *et al.* developed resin formulations combining diacrylate-mediated cross-linking with dithiol-mediated chain transfer and reactive diluents, based on urethan-diacrylate monomers (Fig. 4E). By use of DLP, they

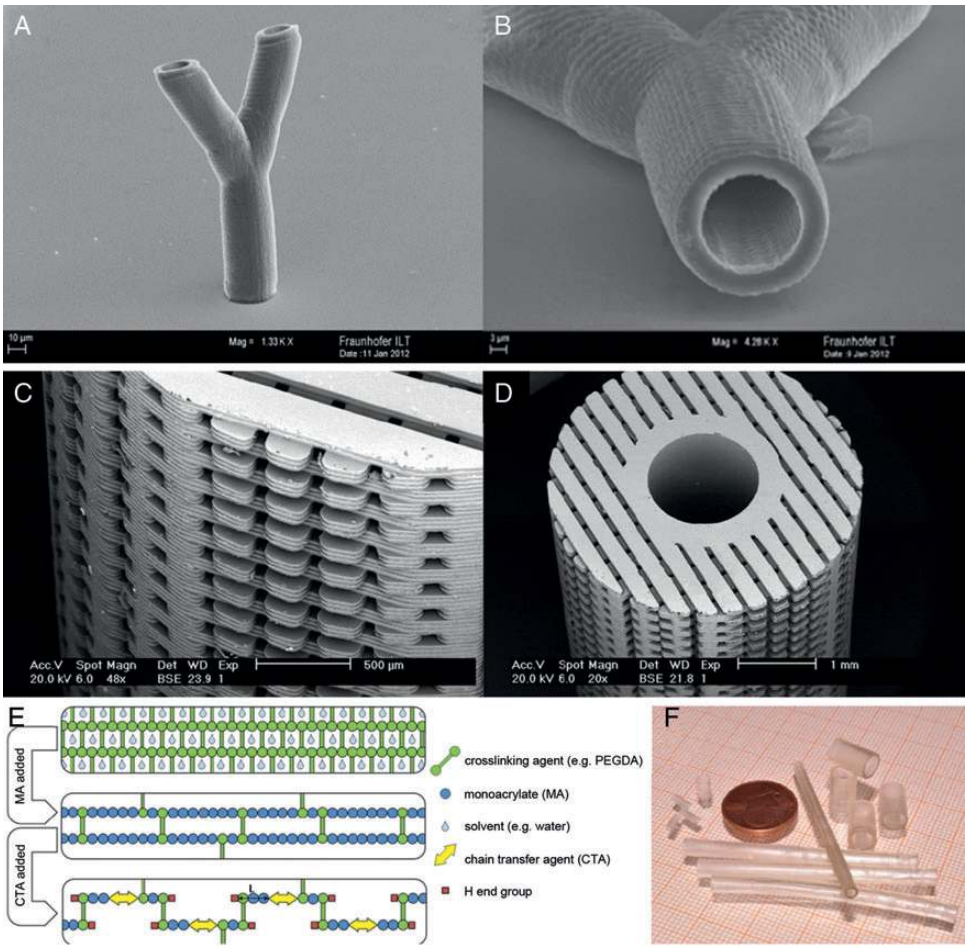

Figure 4: Complex structures, achieved by application of free-form fabrication methods using light-induced cross-linking of polymers. (**A** and **B**) Scanning electron micrographs of branched tubular structure, generated by two-photon polymerization of photo-polymerizable α,ω-polytetrahydrofuranether-diacrylate (PTHF-DA) resins. The height of the tubular structures is ∼160 µm, where the inner diameter and wall thickness are ∼18 and 3 µm, respectively. (Reproduced from Meyer *et al.*, [49] with the permission of the authors.) (**C** and **D**) SEM images of a highly porous CAD–CAM structure out of a cytocompatible photopolymer (from [75]), fabricated by microstereolithography applying a UV laser. (Reproduced from Baudis *et al.* [38] with the permission of IOP Publishing and the authors.) In both cases, the materials proved to be cytocompatible, but do not yet meet the required physicochemical properties for artificial blood vessels. (**E**) Graphical illustration of sophisticated material design. Top: Commonly used hydrogels based on polyethylene glycol diacrylates (PEGDAs) with a high cross-link density along the polymer backbone are sensitive to cracks as they cannot dissipate energy by inter-chain gliding modes. Middle: The addition of reactive diluents based on methacrylate loosens the network as the cross-link density is reduced. Bottom: The application of chain transfer agents was tested in order to change the polymer architecture and to provide relief to the brittle material properties that seem to be an intrinsic property of the poly(acrylate) back bone. (**F**) Tubular structures fabricated from the new formulations based on (**E**) using digital light processing (DLP). (**C** and **D**) reproduced from Baudis *et al.* [38] with the permission of IOP Publishing and the authors). MA: monoacrylate; CTA: chain transfer agent.

generated polymer networks with reduced cross-linking density and high contents of reversible H-bonds (Fig. 4F). Based on the resulting gliding of the polymer chains, they produced tough materials with tensile strength (∼1 MPa), suture tear resistance (∼300 N mm^{-1}) and elastic modulus (<1 MPa) in the range of native porcine carotid arteries.

The first attempts in fabrication of tubular hydrogel structures by drop-on-demand inkjet printing were published by Kesari *et al.*, again from the Boland laboratory in Texas, in 2005. They pursued the approach of printing liquid in liquid, thereby encompassing the challenge of supporting the growing structure: They were the first to exploit the calcium chloride ($CaCl_2$)-based alginate complex formation in inkjet printing by printing $CaCl_2$ solution into an alginate bath using a modified Hewlett Packard printer [53]. As the bivalent Ca-ions mix with the alginate, the alginate polymer is cross-linked into a hydrogel. The authors encapsulated smooth muscle cells into the hydrogel constructs by manually pipetting cell suspensions onto each gel layer before the addition of the next one. The inner diameters, wall thicknesses and heights of the resulting structures were all ∼2 mm, thereby demonstrating the difficulty to control materials and processes in layer-by-layer assembly of high-aspect-ratio structures.

Nakamura and colleagues have reworked the method and succeeded with the preparation of alginate-based tubular structures by applying the reverse process [50–52]. They fabricated fibres and tubes by ejection of alginate droplets into a solution of $CaCl_2$ (Fig. 5A). Just after contact, well-defined hydrogel spheroids form by diffusion of Ca-ions into the alginate ink droplets. Such hydrogel spheroids with semi-solid properties allowed what they called laminating printing, i.e. printing of structures without bleeding. The wall thickness and the inner diameters of tubular structures could be adjusted from 35 to 40 µm and from 30 to 200 µm, respectively, by variation of the diameter of the microgel beads from 10 to 40 µm [50]. The authors additionally improved the morphology of the resulting 3D structures by increasing the viscosity of the $CaCl_2$ substrate bath using hyaluronan or polyvinyl

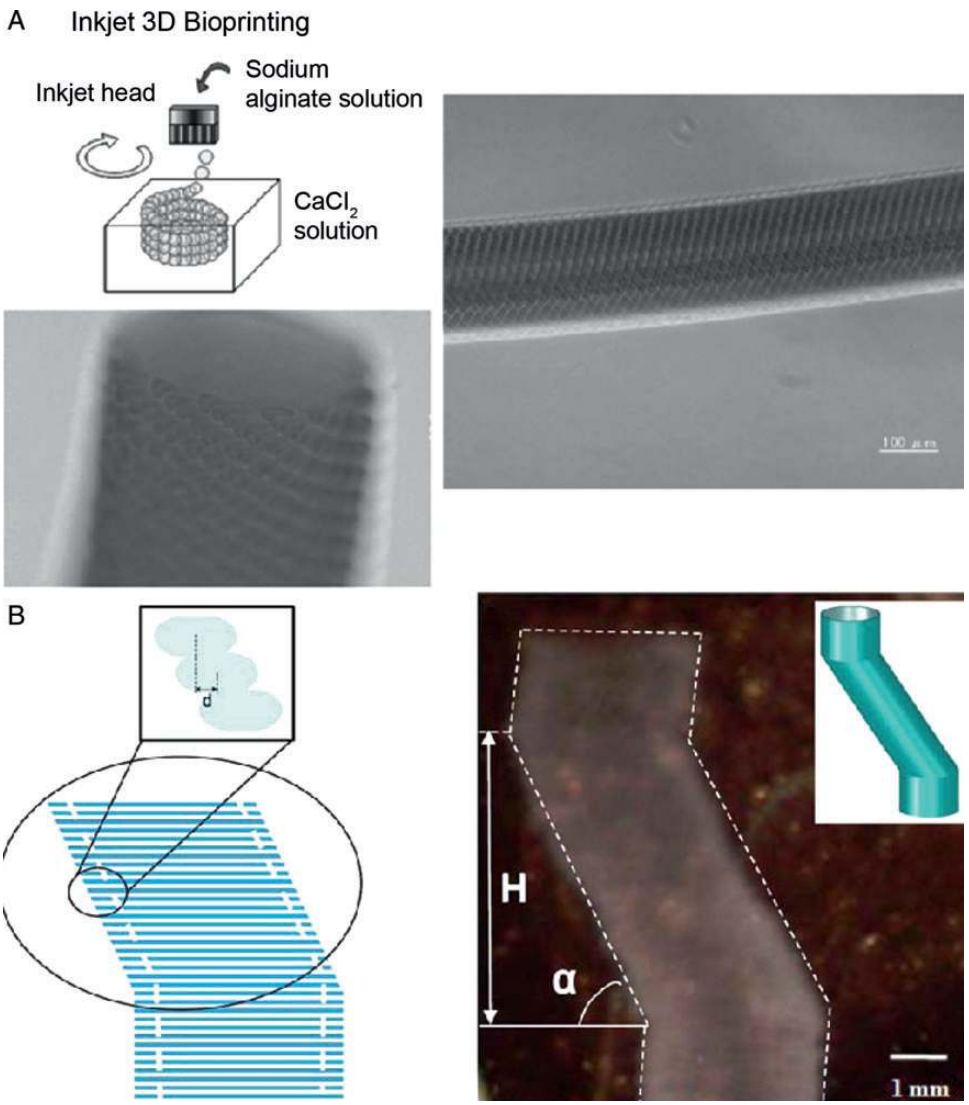

Figure 5: Drop-on-demand assembly of tubes was achieved by printing droplets of alginate bioinks into $CaCl_2$ solutions. (**A**) Very precise 'laminating printing' of tubes without bleeding by fusion of gelling alginate (0.8%) droplets within Ca/polyvinyl alcohol solution. (Reproduced from Nakamura *et al.* [51], with the permission of IS&T: The Society for Imaging Science and Technology, sole copyright owners of *Journal of Imaging Science and Technology*.) (**B**) By the selection of proper printing conditions, scaffold-free zigzag tube printing was achieved in $CaCl_2$ using alginate (1% w/v) bioinks containing fibroblasts. The maximum achievable height depended on the inclination angle of the overhang structure. (Reproduced from Xu *et al.* [54], with the permission of John Wiley and Sons.)

alcohol (PVA). The authors also proved that the generation of cell-laden tubular structures was possible using HeLa cells [52]. With their method, Nakamura *et al.* were able to prepare linear tubular structures with lengths in the centimetre range.

Xu *et al.* have refined the technique and designed a drop-on-demand inkjet-printing process to vertically fabricate 3D zigzag tube structures [54]. By carefully selecting the operating conditions with the help of the buoyant force from the $CaCl_2$ solution, they achieved deposition of 210 layers of Ca-alginate droplets with encapsulated 3T3 fibroblast cells to form the freestanding tube shown in Fig. 5B with a height of 10 mm, an overhang angle of 63° and an overhang height of 5 mm.

These studies show that careful and detailed optimization of the materials and printing processes is necessary in order to exploit the potential of printing and microdispensing for advanced TE in the future. However, alginate is not an ideal material for living tissue construction as it is not part of the natural ECM of mammals and does not promote cell adhesion and tissue growth and, thus apoptosis may be induced in encapsulated cells. In addition, though alginate is known to have a high level of bioaffinity, it is unknown whether it is biodegradable in a human body. Therefore, the use of more ECM-like materials instead of or along with alginate gel is required [76].

Yet, the stacking of droplets or strands is difficult to control and without a stabilizing bath as in the $CaCl_2$-alginate system, adequate supporting materials and structures are needed for free-form fabrication processes. To work in combination with the building materials, such support materials also have to fulfil a long catalogue of requirements, e.g. removability, and the ability to form defined interfaces with building materials, i.e. showing neither repelling effects nor blending. While printing-based techniques have the general advantage that different building materials can be combined within the process of assembly—which is not possible in using cross-linking within a bath—the major challenge of the necessity of supporting free-standing structures currently limits the resolution in nozzle-based or printer-based techniques.

Visser *et al.* [60], have tested combinations of various building materials and support materials in order to improve shape fidelity in generation of complex structures by nozzle-based deposition techniques: Hydrogels which are derived from the natural ECM (gelatin, which is derived from collagen and photo-cross-linkable due to methacrylation (GelMA) together with gellan gum) and Ca-alginate as supportive material; or biodegradable thermoplastic polycaprolactone (PCL) as building material with PVA as a supportive material. They used piston-driven syringes for hydrogel deposition and screw-driven melt extrusion of PCL and PVA. Removal of PVA support structures from PCL was achieved simply by rinsing with water; PCL could be removed from GelMA gels manually and Ca-alginate could be washed away from UV-cured GelMA in sodium citrate solutions. They achieved a free-standing, multi-branched tubular structure fabricated out of PCL strands using PVA support structures in the dimensions of $67 \times 42 \times 8$ mm^3 (L × W × H).The open vessel lumen of the branches decreased from 4 mm to 2 mm in diameter. Such digitally fabricated constructs are rather stiff and could, for example, serve as degradable scaffolds to be integrated into moulded hydrogels to temporarily stabilize biomimetic tube structure for tissue-engineering purposes. The GelMA/gellan hydrogel structures presented by the authors displayed channel diameters of approximately 5 mm and wall thicknesses of 2–5 mm after removal of Ca-alginate sacrificial material. Thus, such bio-based hydrogel material systems were in the same dimensional range as the perfusable matrix structures described earlier rather than near the aspect ratio of tubular structures and, thus, demonstrate once again the difficulty of controlling resolution in bottom-up assembly of hydrogels using drop-on-demand printing.

Similar materials and methods were applied by Skardal and colleagues, who prepared cell-laden tubular structures with lumina in the upper micrometre to millimetre range (0.5–5 mm) applying the nozzle-based system Fab@Home [57–59]. They first printed a central, cell-free core disc using a spiral pattern (1–2 mm), then added a cell-containing ring around the core (2 mm) and finally added another cell-free supportive outer ring. These steps were iterated along the *z*-axis to produce cylindrical structures. In one approach, they used chemically modified, photo-cross-linkable gelatin and photo-cross-linkable hyaluronic acid (HA) as building materials [58]. In another approach, thiol-modified gelatin and thiol-modified HA were cross-linked via multivalent gold nanoparticles [57] or tetra-acrylated polyethylene glycol derivatives [59]. In all cases, the building materials were partially cross-linked prior to printing and further cross-linked after printing, either by UV irradiation or by incubation at 37°C. As supportive material, they used non-cross-linkable HA derivatives. HA does not support cell attachment and thus the non-adhesive surface forced the cells to remain within the desired tubular structure. To obtain free-standing tubes with hollow cavities, the supportive HA was then removed. Although the aspect ratios achieved were again very low, this study proved that providing ECM-derived components within the hydrogel matrix supported the viability of the encapsulated cells, which were then able to remodel the temporary artificial ECM by secretion of endogenous ECM proteins.

Duarte Campos *et al.* [55] presented an interesting approach in combining high-density fluorocarbon as a liquid support material with drop-on-demand printing: They generated high-aspect-ratio hollow fibres by syringe-based dispensing of agarose hydrogels with encapsulated human mesenchymal stem cells (hMSCs). As the contact angle of agarose gel droplets printed onto the hydrophilic surface of the cross-linked gel was increased within the hydrophobic environment, the precision of the printing was increased. Histological analyses after 21 days proved cells to be viable with marked matrix production within the constructs. Thus, for the cell types used (hMSCs and human MG-63 cells, an osteosarcoma-derived cell line), it is suggested that the polysaccharide agarose served as an adequate temporary matrix and that the fluorocarbon support did not significantly harm the encapsulated cells.

Another aspect in view of future reconstruction of native blood vessels was captured by Kucukgul *et al.* [77], who have captured the geometry of an aorta from magnetic resonance imaging data and have then segmented and converted them into 3D computer models. Yet, due to the above-mentioned difficulties in stabilizing their constructs, the authors have presented the proof of their data conversion by an eight-layer model only.

Very straightforward approaches also introduced direct extrusion of hollow fibres using coaxial nozzles. While this method cannot provide any branched tubular structures, perfusion systems for 3D cell culture or even fabrication of small-diameter vascular grafts for medical applications may be achieved in the future. Luo *et al.* from the Gelinsky laboratory have applied the Ca-alginate system for the production of stacks of inter-bred hollow fibres [78]. They generated freestanding hollow fibres by continuous extrusion of highly concentrated alginate (16.7% w/w) with PVA (6% w/v) solution using a home-built shell/core nozzle tip. After extrusion, the scaffolds were transferred to $CaCl_2$ solution in order to achieve the complexion of the alginate and dissolution of the PVA. The outer and inner

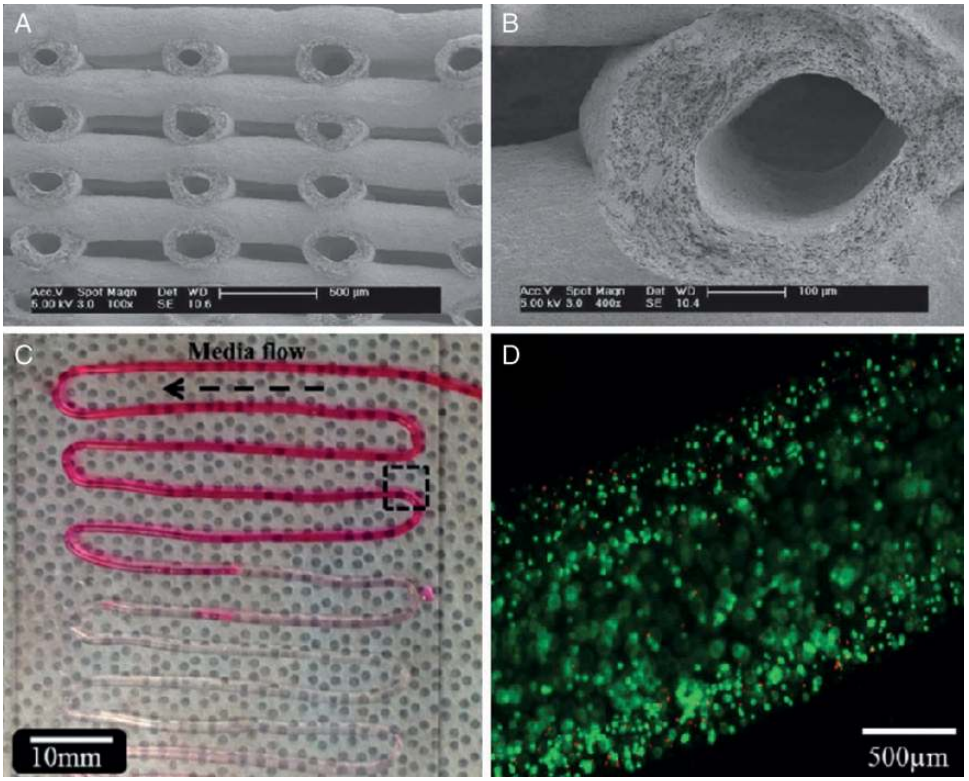

Figure 6: Plotting of hollow fibres by the use of core/shell nozzles directly provided vessel-like perfusable tubes for developing embedded channels serving as a vascular network for thick tissue fabrication. (**A** and **B**) plotted alginate/polyvinyl alcohol scaffold consisting of layers of hollow strands. (Reproduced from Luo *et al.* [78], with permission of John Wiley and Sons.) (**C**) Media perfusion through an alginate microfluidic channel, 44 cm in length and 1 mm in width with 500-µm lumen diameter. (**D**) Cartilage cells were encapsulated in the hydrogel solution during the extrusion process (green fluorescence: viable cells, red: dead cells). (Reproduced from Zhang *et al.* [64] with permission of the American Society of Mechanical Engineers (ASME).).

diameters of the hollow fibres were adjusted to 300–1000 and 150–450 µm, respectively, and multilayer stacks were prepared (Fig. 6A and B).

A similar approach was introduced by Zhang, Yu and Ozbolat (Fig. 6C and D). They fabricated hollow tubes without support by dispensing less concentrated (2–6%), cell-laden sodium alginate through the outer tube of a coaxial nozzle system with simultaneously flushing of $CaCl_2$ cross-linker solution through the inner tube [62–64]. They also tested chitosan and sodium hydroxide solution with less success. In their study, the authors used cartilage progenitor cells and reported that, depending on process and material parameters such as nozzle diameters, dispensing pressure and alginate concentration, the viability of the encapsulated cells dropped significantly at early time points after printing but recovered over the time course of 72 h. This suggests that, for the specific cell type—cartilage cells generally display spherical morphology, without distinct adhesion to the surrounding matrix—alginate-based matrices might act as adequate matrix material.

As all scaffold-based biomaterials have to deal with challenges such as cyto- and biocompatibility, degradation behaviour or potential immunogenicity, Norotte and Jakab from the Forgacs laboratory, which is also the origin of the bioprinting, and bioengineering companies Organovo (Organovo Holdings, Inc., CA, USA) and Modern Meadow (Modern Meadow LLC, Columbia, MO, USA), finally focus on fabrication of scaffold-free tissue constructs based only on cells and the genuine matrix they secrete. They applied one-by-one bioplotting of cell aggregates consisting of either one cell type or several cell types for the fabrication of tubular structures [61, 71]. In a first approach, vertical tubes were fabricated by alternate deposition of the spherical cell aggregates and collagen, which served as sacrificial supporting material. The cell spheroids fused within 5–7 days into stable tubular structures and, thus, after removal of the stabilizing collagen sheets, hollow tubes were achieved. One limitation of this early approach was that the supportive collagen layers could not be completely removed since cells integrated the collagen into the final structure. Thus, in a second approach, they replaced collagen with agarose, which is biologically inert and cannot be invaded or rearranged by cells. Moreover, they found that, instead of tissue spheroids, the use of multicellular cylinders represented considerable progress in terms of time and precision of the final structure. By combination of multicellular cylinders made from HUVSMCs and human dermal fibroblasts (HDFs), double-layered vascular walls could be built. The fused artificial vessels were sufficiently sturdy to be handled and transferred into specifically designed bioreactors for further maturation. In these studies, the smallest tube achieved was 90 µm in diameter and obtained a wall thickness of 300 µm. This approach is particularly interesting because vessel walls based on the modelling activities of the cells are achieved.

CONCLUSION

The generation of vascularized tissue is one of the key challenges in TE. The evaluation of free-form fabrication methods for the generation of perfusable tissue is an important step towards this demanding goal.

From our current point of view, the fabrication of perfusable channel systems within cell-laden hydrogel matrices has proved to be the most straightforward method to generate large 3D tissue constructs by enabling the exchange of O_2 and CO_2, and nutrient supply within the 3D matrix bulk. This approach allows fulfillment of the initially recognized requirements of both, defined inlet and outlet branches connected to a channel network with biomimetic geometry for undisturbed fluid dynamics, and the conditions for formation of new capillaries through angiogenesis. Thus, we expect this approach to be the crucial next step that will initiate real 3D TE.

First proofs of concept showed that cartridge-based drop-on-demand techniques can be expected to be of great use for the combination of different matrices and cells in a 3D organized manner as required for biomimetic assembly of tissue. Yet, they seem to be limited for assembly of freestanding high-aspect-ratio structures.

Extrusion of hollow fibres does not provide the full range of degrees of freedom that are connected to free-form fabrication methods, yet we appreciate the method to be straightforward for preparation of linear channels and also for basic supply of 3D tissue models. Additionally, the presented approaches strongly feed our vision of completely new generation of vessel substitutions for cardiovascular diseases. Yet, numerous challenges have to be met and very accurate developments in materials science are needed, whether based on synthetic or biological polymers, in order to match the mechanical and biological properties of native vessels such as compliance, tear strength, bursting strength, haemocompatibility and long-term stability. The full structure and function may even be established by integrated cells remodelling the bioartificial vessel wall. Thus, we assume that 5–10 years of research and development are additionally needed to achieve the demanding goal of bioprinting blood vessels for the first *in vivo* trials.

ACKNOWLEDGEMENTS

The authors thank the Fraunhofer Gesellschaft, the European Commission (Artivasc 3D GA 263 416), and the Peter und Traudl Engelhorn Stiftung for financial support.

Conflict of interest: none declared.

REFERENCES

[1] Langer R, Vacanti J. Tissue engineering. Science 1993;260:920–6.
[2] De Kanter R, Olinga P, De Jager MH, Merema MT, Meijer DKF, Groothius GMM. Organ slices as an in vitro test system for drug metabolism in human liver, lung and kidney. Toxicol In Vitro 1999;13:737–44.
[3] Henmi C, Nakamura M, Nishiyama Y, Yamaguchi K, Mochizuki S, Takiura K *et al*. Development of an effective three dimensional fabrication technique using inkjet technology for tissue model samples. In: AATEX 14 Proceedings of 6th World Congress on Alternatives & Animal Use in Life Sciences. Tokyo: Japanese Society for Alternatives to Animal Experiments, 2007;689–92.
[4] Risbud MV, Sittinger M. Tissue engineering: advances in in vitro cartilage generation. Trends Biotechnol 2002;20:351–6.
[5] Hou N. Tissue-engineered trachea using perfusion-decellularized technique and mesenchymal stem cells in a rabbit model. J Neurol Surg B 2012;73:438–43.
[6] Ott HC, Matthiesen TS, Goh S-K, Black LD, Kren SM, Netoff TI *et al*. Perfusion-decellularized matrix: using nature's platform to engineer a bioartificial heart. Nat Med 2008;14:213–21.
[7] Uygun BE, Soto-Gutierrez A, Yagi H, Izamis M-L, Guzzardi MA, Shulman C *et al*. Organ reengineering through development of a transplantable recellularized liver graft using decellularized liver matrix. Nat Med 2010;16:814–20.
[8] Price AP, England KA, Matson AM, Blazar BR, Panoskaltsis-Mortari A. Development of a decellularized lung bioreactor system for bioengineering the lung: the matrix reloaded. Tissue Eng Part A 2010;16:2581–91.
[9] Freyman TM, Yannas IV, Gibson LJ. Cellular materials as porous scaffolds for tissue engineering. Prog Mater Sci 2001;46:273–82.
[10] Mikos AG, Temenoff JS. Formation of highly porous biodegradable scaffolds for tissue engineering. Electron J Biotechnol 2000;3:1–6.
[11] Lannutti J, Reneker D, Ma T, Tomasko D, Farson D. Electrospinning for tissue engineering scaffolds. Mater Sci Eng C 2007;27:504–9.
[12] Sachlos E, Czernuszka JT. Making tissue engineering scaffolds work. Review: the application of solid freeform fabrication technology to the production of tissue engineering scaffolds. Eur Cell Mater 2003;5:29–39.
[13] Hoffman AS. Hydrogels for biomedical applications. Adv Drug Deliv Rev 2012;64:18–23.
[14] Hunt N, Grover L. Cell encapsulation using biopolymer gels for regenerative medicine. Biotechnol Lett 2010;32:733–42.
[15] Nicodemus GD, Bryant SJ. Cell encapsulation in biodegradable hydrogels for tissue engineering applications. Tissue Eng 2008;14:149–65.
[16] Lee W, Debasitis JC, Lee VK, Lee J-H, Fischer K, Edminster K *et al*. Multi-layered culture of human skin fibroblasts and keratinocytes through three-dimensional freeform fabrication. Biomaterials 2009;30:1587–95.
[17] Yang EK, Seo YK, Youn HH, Lee DH, Park SN, Park JK. Tissue engineered artificial skin composed of dermis and epidermis. Artif Organs 2000;24:7–17.
[18] Benders KEM, Weeren PRv, Badylak SF, Saris DBF, Dhert WJA, Malda J. Extracellular matrix scaffolds for cartilage and bone regeneration. Trends Biotechnol 2013;31:169–76.
[19] Temenoff JS, Mikos AG. Review: tissue engineering for regeneration of articular cartilage. Biomaterials 2000;21:431–40.
[20] Sabater AL, Guarnieri A, Espana EM, Li W, Prosper F, Moreno-Montanes J. Strategies of human corneal endothelial tissue regeneration. Regen Med 2013;8:183–95.
[21] Kuo CK, Li W-J, Mauck RL, Tuan RS. Cartilage tissue engineering: its potential and uses. Curr Opin Rheumatol 2006;18:64–73.
[22] Schulz RM, Bader A. Cartilage tissue engineering and bioreactor systems for the cultivation and stimulation of chondrocytes. Eur Biophys J 2007;36:539–68.
[23] Novosel EC, Kleinhans C, Kluger PJ. Vascularization is the key challenge in tissue engineering. Adv Drug Deliv Rev 2011;63:300–11.
[24] Tortorra GJD. Anatomie und Physiologie. Weinheim: Wiley-VHC, 2006.
[25] Kamiya A, Togawa T. Optimal branching structure of the vascular tree. Bull Math Biophys 1972;34:431–8.
[26] Moya ML, Hsu Y-H, Lee AP, Hughes CCW, George SC. In vitro perfused human capillary networks. Tissue Eng Part C Methods 2013;19:730–7.
[27] Tremblay PL, Hudon V, Berthod F, Germain L, Auger FA. Inosculation of tissue-engineered capillaries with the host´s vasculature in a reconstructed skin transplanted on mice. Am J Transplant 2005;5:1002.
[28] Nunes SS, Krishnan L, Gerard CS, Dale JR, Maddie MA, Benton RL *et al*. Angiogenic potential of microvessel fragments is independent of the tissue of origin and can be influenced by the cellular composition of the implants. Microcirculation 2010;17:557–67.
[29] Kannan RY, Salacinski HJ, Sales K, Butler P, Seifalian AM. The roles of tissue engineering and vascularisation in the development of micro-vascular networks: a review. Biomaterials 2005;26:1857–75.
[30] Scheller K. Upcyte(R) microvascular endothelial cells repopulate decellularized scaffold. Tissue Eng Part C Methods 2013;19:57–67.
[31] Novosel EC, Meyer W, Klechowitz N, Krüger H, Wegener M, Walles H *et al*. Evaluation of cell-material interactions on newly designed, printable polymers for tissue engineering applications. Adv Eng Mater 2011;13:B467–75.
[32] Tsang VL, Bhatia SN. Three-dimensional tissue fabrication. Adv Drug Deliv Rev 2004;56:1635–47.
[33] Guillemot F, Mironov V, Nakamura M. Bioprinting is coming of age: report from International Conference on Bioprinting and Biofabrication in Bordeaux (3B'09). Biofabrication 2010;2:1–7.
[34] Melchels FPW, Domingos MAN, Klein TJ, Malda J, Bartolo PJ, Hutmacher DW. Additive manufacturing of tissues and organs. Prog Polym Sci 2012;37:1079–104.
[35] Wüst S, Müller R, Hofmann S. Controlled positioning of cells in biomaterials—approaches towards 3D tissue printing. J Funct Biomater 2011;2:119–54.
[36] Chang CC, Boland ED, Williams SK, Hoying JB. Direct-write bioprinting three-dimensional biohybrid systems for future regenerative therapies. J Biomed Mater Res B Appl Biomater 2011;98B:160–70.

[37] Hoch E, Hirth T, Tovar GEM, Borchers K. Chemical tailoring of gelatin to adjust its chemical and physical properties for functional bioprinting. J Mater Chem B 2013;1:5675–85.
[38] Baudis S, Nehl F, Ligon SC, Nigisch A, Bergmeister H, Bernhard D *et al*. Elastomeric degradable biomaterials by photopolymerization-based CAD-CAM for vascular tissue engineering. Biomed Mater 2011;6:055003.
[39] Engelhardt S, Hoch E, Borchers K, Meyer W, Krüger H, Tovar G *et al*. Fabrication of 2D protein microstructures and 3D polymer–protein hybrid microstructures by two-photon polymerization. Biofabrication 2011;3:025003.
[40] Bellan LM, Pearsall M, Cropek DM, Langer R. A 3D interconnected microchannel network formed in gelatin by sacrificial shellac microfibers. Adv Mater 2012;24:5187–91.
[41] Miller JS, Stevens KR, Yang MT, Baker BM, Nguyen D-HT, Cohen DM *et al*. Rapid casting of patterned vascular networks for perfusable engineered three-dimensional tissues. Nat Mater 2012;11:768–74.
[42] Wu W, DeConinck A, Lewis JA. Omnidirectional printing of 3D microvascular networks. Adv Mater 2011;23:H178–83.
[43] Lee W, Lee V, Polio S, Keegan P, Lee JH, Fischer K *et al*. On-demand three-dimensional freeform fabrication of multi-layered hydrogel scaffold with fluidic channels. Biotechnol Bioeng 2010;105:1178–86.
[44] Li S, Xiong Z, Wang X, Yan Y, Liu H, Zhang J. Direct fabrication of a hybrid cell/hydrogel construct by a double-nozzle assembling technology. J Bioact Compat Polym 2009;24:249–65.
[45] Wu PK, Ringeisen BR. Development of human umbilical vein endothelial cell (HUVEC) and human umbilical vein smooth muscle cell (HUVSMC) branch/stem structures on hydrogel layers via biological laser printing (BioLP). Biofabrication 2010;2:014111–119.
[46] Guillotin B, Souquet A, Catros S, Duocastella M, Pippenger B, Bellance S *et al*. Laser assisted bioprinting of engineered tissue with high cell density and microscale organization. Biomaterials 2010;31:7250–6.
[47] Cui X, Boland T. Human microvasculature fabrication using thermal inkjet printing technology. Biomaterials 2009;30:6221–7.
[48] Chang CC, Krishnan L, Nunes SS, Church KH, Edgar LT, Boland ED *et al*. Determinants of microvascular network topologies in implanted neovasculatures. Arterioscler Thromb Vasc Biol 2012;32:5–14.
[49] Meyer W, Engelhardt S, Novosel E, Elling B, Wegener M, Krüger H. Soft Polymers for building up small and smallest blood supplying systems by stereolithography. J Funct Biomater 2012;3:257–68.
[50] Nakamura M, Nishiyama Y, Henmi C. 3D micro-fabrication by inkjet 3D biofabrication for 3D tissue engineering. In: Proceedings of the International Symposium on Micro-NanoMechatronics and Human Science. New York, USA: Institute of Electrical and Electronics Engineers IEEE, 2008;451–6.
[51] Nakamura M, Nishiyama Y, Henmi C, Iwanaga S, Nakagawa H. Ink jet three-dimensional digital fabrication for biological tissue manufacturing: analysis of alginate microgel beads produced by ink jet droplets for three dimensional tissue fabrication. J Imaging Sci Technol 2008;52:1–16.
[52] Nishiyama Y, Nakamura M, Henmi C, Yamaguchi K, Mochizuki S, Nakagawa H *et al*. Development of a three-dimensional bioprinter: construction of cell supporting structures using hydrogel and state-of-the-art inkjet technology. J Biomech Eng 2009;131:1–6.
[53] Kesari P, Xu T, Boland T. Layer-by-layer printing of cells and its application to tissue engineering. Nanoscale Mater Sci Biol Med 2005;845:111–7.
[54] Xu C, Chai W, Huang Y, Markwald RR. Scaffold-free inkjet printing of three-dimensional zigzag cellular tubes. Biotechnol Bioeng 2012;109:3152–60.
[55] Duarte Campos DF, Blaeser A, Weber M, Jäkel J, Neuss S, Jahnen-Dechent W *et al*. Three-dimensional printing of stem cell-laden hydrogels submerged in a hydrophobic high-density fluid. Biofabrication 2013;5:015003–014.
[56] Kucukgul C, Ozler B, Karakas HE, Gozuacik D, Koc B. 3D Hybrid bioprinting of macrovascular structures. Proc Eng 2013;59:183–92.
[57] Skardal A, Zhang J, McCoard L, Oottamasathien S, Prestwich GD. Dynamically crosslinked gold nanoparticle–hyaluronan hydrogels. Adv Mater 2010;22:4736–40.
[58] Skardal A, Zhang J, McCoard L, Xu X, Oottamasathien S, Prestwich GD. Photocrosslinkable hyaluronan-gelatin hydrogels for two-step bioprinting. Tissue Eng Part A 2010;16:2675–85.
[59] Skardal A, Zhang J, Prestwich GD. Bioprinting vessel-like constructs using hyaluronan hydrogels crosslinked with tetrahedral polyethylene glycol tetracrylates. Biomaterials 2010;31:6173–81.
[60] Visser J, Peters B, Burger TJ, Boomstra J, Dhert WJ, Melchels FP *et al*. Biofabrication of multi-material anatomically shaped tissue constructs. Biofabrication 2013;5:1–9.
[61] Norotte C, Marga FS, Niklason LE, Forgacs G. Scaffold-free vascular tissue engineering using bioprinting. Biomaterials 2009;30:5910–7.
[62] Yu Y, Zhang Y, Martin JA, Ozbolat IT. Evaluation of cell viability and functionality in vessel-like bioprintable cell-laden tubular channels. J Biomech Eng 2013;135:91011.
[63] Zhang Y, Yu Y, Chen H, Ozbolat IT. Characterization of printable cellular micro-fluidic channels for tissue engineering. Biofabrication 2013;5:025004.
[64] Zhang Y, Yu Y, Ozbolat IT. Direct bioprinting of vessel-like tubular microfluidic channels. J Nanotechnol Eng Med 2013;4:021001-1–021001-7.
[65] Golden AP, Tien J. Fabrication of microfluidic hydrogels using molded gelatin as a sacrificial element. Lab Chip 2007;7:720–5.
[66] Choi NW, Cabodi M, Held B, Gleghorn JP, Bonassar LJ, Stroock AD. Microfluidic scaffolds for tissue engineering. Nat Mater 2007;6:908–15.
[67] Ling Y, Rubin J, Deng Y, Huang C, Demirci U, Karp JM *et al*. A cell-laden microfluidic hydrogel. Lab Chip 2007;7:756–62.
[68] Abdi S, Choi J, Lee J, Lim H, Lee C, Kim J *et al*. In vivo study of a blended hydrogel composed of pluronic F-127-alginate-hyaluronic acid for its cell injection application. Tissue Eng Regen Med 2012;9:1–9.
[69] Khattak SF, Bhatia SR, Roberts SC. Pluronic F127 as a cell encapsulation material: utilization of membrane-stabilizing agents. Tissue Eng 2005;11:974–83.
[70] Thonhoff JR, Lou DI, Jordan PM, Zhao X, Wu P. Compatibility of human fetal neural stem cells with hydrogel biomaterials in vitro. Brain Res 2008;1187:42–51.
[71] Jakab K, Norotte C, Marga F, Murphy K, Vunjak-Novakovic G, Forgacs G. Tissue engineering by self-assembly and bio-printing of living cells. Biofabrication 2010;2:022001.
[72] Cascone I, Giraudo E, Caccavari F, Napione L, Bertotti E, Collard JG *et al*. Temporal and spatial modulation of Rho GTPases during in vitro formation of capillary vascular network: adherens junctions and myosin light chain as targets of Rac1 and RhoA. J Biol Chem 2003;278:50702–13.
[73] Korff T, Kimmina S, Martiny-Baron G, Augustin HG. Blood vessel maturation in a 3-dimensional spheroidal coculture model: direct contact with smooth muscle cells regulates endothelial cell quiescence and abrogates VEGF responsiveness. FASEB J 2001;15:447–57.
[74] Darland DC, Massingham LJ, Smith SR, Piek E, Saint-Geniez M, D'Amore PA. Pericyte production of cell-associated VEGF is differentiation-dependent and is associated with endothelial survival. Dev Biol 2003;264:275–88.
[75] Schuster M, Turecek C, Kaiser B, Stampfl J, Liska R, Varga F. Evaluation of biocompatible photopolymers I: photoreactivity and mechanical properties of reactive diluents. J Macromol Sci Part A 2007;44:547–57.
[76] Nakamura M, Iwanaga S, Henmi C, Arai K, Nishiyama Y. Biomatrices and biomaterials for future developments of bioprinting and biofabrication. Biofabrication 2010;2:014110–116.
[77] Kucukgul C, Ozler B, Karakas HE, Gozuacik D, Koc B. 3D hybrid bioprinting of macrovascular structures. Procedia Engineering 2013;59:183–92.
[78] Luo Y, Lode A, Gelinsky M. Direct plotting of three-dimensional hollow fiber scaffolds based on concentrated alginate pastes for tissue engineering. Adv Healthcare Mater 2013;2:777–83.